

Small-scale structure of two-dimensional magnetohydrodynamic turbulence

By STEVEN A. ORSZAG AND CHA-MEI TANG†

Department of Mathematics, Massachusetts Institute of Technology, Cambridge

(Received 6 October 1977)

The formation of singularities in two-dimensional magnetohydrodynamic flow is investigated by direct numerical simulation. It is shown that two-dimensional magnetohydrodynamic turbulence is not as singular as three-dimensional hydrodynamic turbulence (in the sense that it has a less highly excited small-scale structure) but that it is more singular than two-dimensional hydrodynamic turbulence.

1. Introduction

Two-dimensional magnetohydrodynamic (MHD) turbulence has been the subject of much recent research interest (Fyfe & Montgomery 1976; Fyfe, Joyce & Montgomery 1977; Pouquet 1978; Weiss 1966). In this paper, we compare the results of numerical simulations of two- and three-dimensional hydrodynamic and magnetohydrodynamic flows at high Reynolds numbers.

Pouquet (1978) suggests that two-dimensional MHD turbulence is dynamically very similar to three-dimensional hydrodynamic turbulence. She uses an analytical theory of turbulence (the eddy-damped quasi-normal (EDQN) approximation) to infer that small scales are typically excited at a much higher level in two-dimensional MHD turbulence than in two-dimensional hydrodynamic turbulence. In contrast to the inviscid two-dimensional Navier–Stokes (Euler) equations, which are known to have smooth solutions for all time (Wolibner 1933; Frisch & Bardos 1975, unpublished), the EDQN approximation suggests that the inviscid two-dimensional MHD equations develop singularities in a finite time, even with periodic boundary conditions and smooth initial conditions. These flow singularities suggest that the small-scale structure of two-dimensional MHD flow is more intermittent than the small-scale structure of two-dimensional hydrodynamic flow.

In this paper, we provide some numerical support for some of Pouquet's conjectures. While we conclude that two-dimensional MHD flow is significantly *less* singular than three-dimensional hydrodynamic flow, we also conclude that it is much *more* singular than two-dimensional hydrodynamic flow. Roughly speaking, two-dimensional magnetohydrodynamic flow behaves like hydrodynamic turbulence in a dimension intermediate between two and three.

† Present address: Jaycor, Alexandria, Virginia.

2. Dynamical equations and numerical methods

The two-dimensional equations of motion for an incompressible conducting fluid in the MHD approximation can be written in terms of the velocity \mathbf{v} , magnetic field \mathbf{h} , vorticity $\zeta \hat{\mathbf{i}}_z = \nabla \times \mathbf{v}$, current $j \hat{\mathbf{i}}_z = \nabla \times \mathbf{h}$ and magnetic vector potential $\mathbf{A} = A \hat{\mathbf{i}}_z$, where $\mathbf{h} = \nabla \times \mathbf{A}$. All variables are functions of x , y and t , and $\hat{\mathbf{i}}_z$ is a unit vector in the z direction. The equations of motion are

$$\partial \zeta / \partial t = -\mathbf{v} \cdot \nabla \zeta + \mathbf{h} \cdot \nabla j + \nu \nabla^2 \zeta, \quad (1)$$

$$\partial A / \partial t = -\mathbf{v} \cdot \nabla A + \mu \nabla^2 A, \quad (2)$$

$$\nabla \cdot \mathbf{h} = 0, \quad \nabla \cdot \mathbf{v} = 0, \quad (3)$$

where ν is the kinematic viscosity and μ is the magnetic diffusivity. In this paper, (1)–(3) are solved with periodic boundary conditions in a box with sides 2π . Thus all fields may be represented as discrete Fourier series with integral wave-vector components.

Equations (1)–(3) with $\nu = \mu = 0$ possess three quadratic constants of motion: the total energy

$$E = \frac{1}{2} \int (|\mathbf{v}|^2 + |\mathbf{h}|^2) d\mathbf{x},$$

the mean-square magnetic vector potential

$$\int A^2 d\mathbf{x}$$

and the cross-helicity

$$\int (\mathbf{v} \cdot \mathbf{h}) d\mathbf{x}.$$

Here we use the notation

$$\int d\mathbf{x} = (2\pi)^{-2} \int_0^{2\pi} dx \int_0^{2\pi} dy.$$

When $\nu > 0$ or $\mu > 0$, the rate of total energy dissipation is given by

$$\epsilon(t) = -dE/dt = \nu \int \zeta^2 d\mathbf{x} + \mu \int j^2 d\mathbf{x}. \quad (4)$$

We use definitions of length scales and Reynolds numbers which follow those used in studies of two-dimensional hydrodynamic turbulence (see Herring *et al.* 1974). The kinetic Reynolds number R^v is defined by

$$R^v = E^v [2 \Sigma k^4 E^v(k)]^{-\frac{1}{2}} \nu^{-\frac{1}{2}} \quad (5)$$

and the magnetic Reynolds number R^m is defined by

$$R^m = E^m [2 \Sigma k^4 E^m(k)]^{-\frac{1}{2}} \mu^{-\frac{1}{2}}. \quad (6)$$

Here $E^v(k)$ and $E^m(k)$ are the kinetic and magnetic energies, respectively, at wave-number k and $E^v = \Sigma E^v(k)$ and $E^m = \Sigma E^m(k)$.

We solved (1)–(3) numerically using the pseudospectral method with a truncated Fourier series expansion of the flow variables (see Gottlieb & Orszag 1977, chap. 2). The computer code was a modification of the KILOBOX code used for high resolution two-dimensional turbulence calculations (Orszag 1976); in this code, up to 1024×1024 modes can be used to represent each dynamical variable at each instant of time. The MHD version of KILOBOX is so designed that only 9 Fourier transforms are required for each time step (Tang 1977). With 256×256 modes, the running time for the present

MHD calculation is about 6 s per time step on a CDC7600. Most of the calculations reported below involve several hundred time steps. The accuracy of our numerical results has been carefully checked as discussed by Herring *et al* (1974). For example, the accuracy of the energy dissipation results plotted in figures 1 and 2 is better than 1 % (Tang 1977).

3. Results

In this section, we report results for the evolution of two-dimensional MHD turbulence with both non-random and random initial conditions. A simple non-random initial condition imposed at $t = 0$ is

$$\mathbf{v} = (-\sin y, \sin x), \quad A = \cos y + \frac{1}{2} \cos 2x. \quad (7)$$

As t increases, this simple flow becomes increasingly complicated owing to the nonlinear interactions in (1)–(3). An analytical solution of (1)–(3) with these initial conditions does not seem possible. With $\nu = \mu = 0.01$, the numerical simulation is accurate at all dynamically important scales with 128×128 Fourier modes; when $\nu = \mu = 0.005$, 256×256 modes are required. When $\nu = \mu \geq 0.02$, accurate results are obtained with 64×64 Fourier modes. For reference, we note that the initial values of the Reynolds numbers R^v and R^m are 232 and 114, respectively, when $\nu = \mu = 0.02$. Both R^v and R^m increase by a factor of $2^{\frac{1}{2}} \doteq 2.52$ when $\nu = \mu$ is halved. Results are presented below for magnetic Prandtl numbers ν/μ equal to $\frac{1}{2}$, 1, and 2.

In figure 1, we plot the total energy dissipation $\epsilon(t)$ *vs.* t for $\nu = \mu = 0.08, 0.04, 0.02, 0.01$ and 0.005 . When $\nu = \mu$ is halved with the fixed initial condition (7), the peak of the energy dissipation rate is decreased by about 20 %.

In figure 2, we plot the evolution of $\epsilon(t)$ *vs.* t when the initial flow is chosen as a realization of a Gaussian ensemble with energy spectrum.

$$E^m(k) = E^v(k) = \frac{2}{3} k e^{-\frac{1}{3}k}. \quad (8)$$

As shown in figure 2, when $\nu = \mu = 0.01$ the peak of the energy dissipation is about 26 % smaller than when $\nu = \mu = 0.02$.

The behaviour exhibited by two-dimensional MHD flow in figures 1 and 2 is quite different from the behaviour of two-dimensional hydrodynamic flow. In two-dimensional hydrodynamics, nonlinear interaction conserves mean-square vorticity (enstrophy), so that the dissipation rate in unforced dissipative turbulence satisfies $\epsilon(t) \leq \epsilon(0)$ for $t \geq 0$. In contrast, $\epsilon(t)/\epsilon(0)$ can achieve values much larger than one in MHD flow.

Comparison of the results plotted in figures 1 and 2 with similar results for three-dimensional hydrodynamics is also instructive. In figure 3 we plot the kinetic energy dissipation $\epsilon(t)$ *vs.* t for the Taylor–Green vortex (Orszag 1977). The initial flow for this vortex motion is

$$\mathbf{v} = (\cos x \sin y \cos z, -\sin x \cos y \cos z, 0).$$

As shown in figure 3, when ν decreases by a factor of 4 (i.e. Reynolds number increases by a factor of 4) the peak in $\epsilon(t)$ changes by about 10 %. The results plotted in figure 3 support the hypotheses (Orszag 1977) that (i) the inviscid three-dimensional Navier–Stokes equations can develop singularities in a finite time and (ii) the rate of kinetic

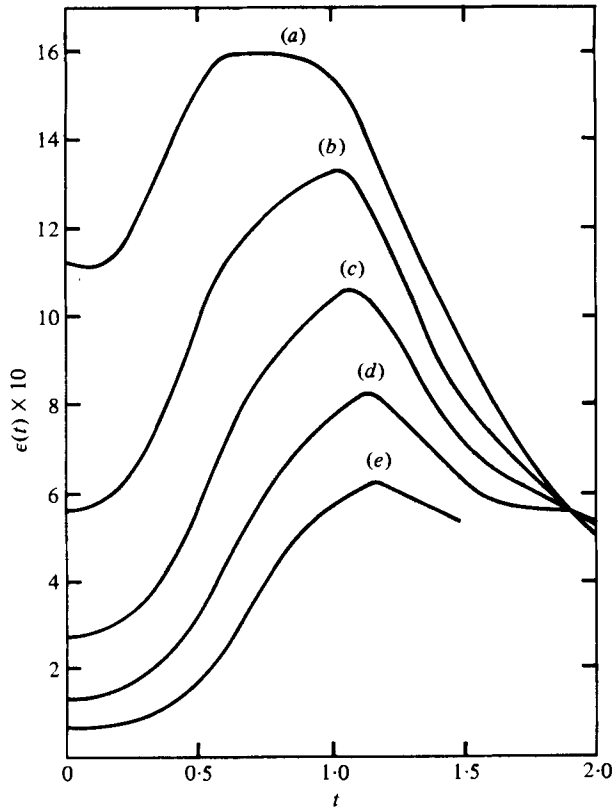


FIGURE 1. A plot of the energy dissipation rate $\epsilon(t)$ of the two-dimensional MHD flow with initial condition (7). (a) $\nu = \mu = 0.08$ ($R^v = 36$), (b) $\nu = \mu = 0.04$ ($R^v = 92$), (c) $\nu = \mu = 0.02$ ($R^v = 232$), (d) $\nu = \mu = 0.01$ ($R^v = 585$), (e) $\nu = \mu = 0.005$ ($R^v = 1474$).

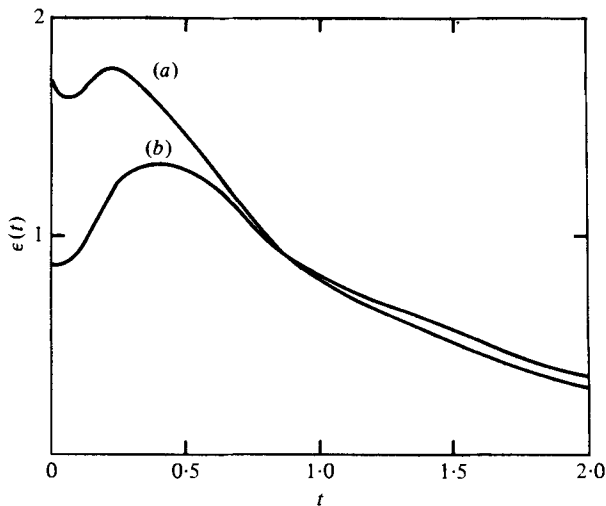


FIGURE 2. A plot of the energy dissipation rate $\epsilon(t)$ for two-dimensional MHD turbulence. The initial flow is chosen as a realization of the Gaussian ensemble with energy spectrum (8). (a) $\nu = \mu = 0.02$ ($R^v = 167$), (b) $\nu = \mu = 0.01$ ($R^v = 420$).

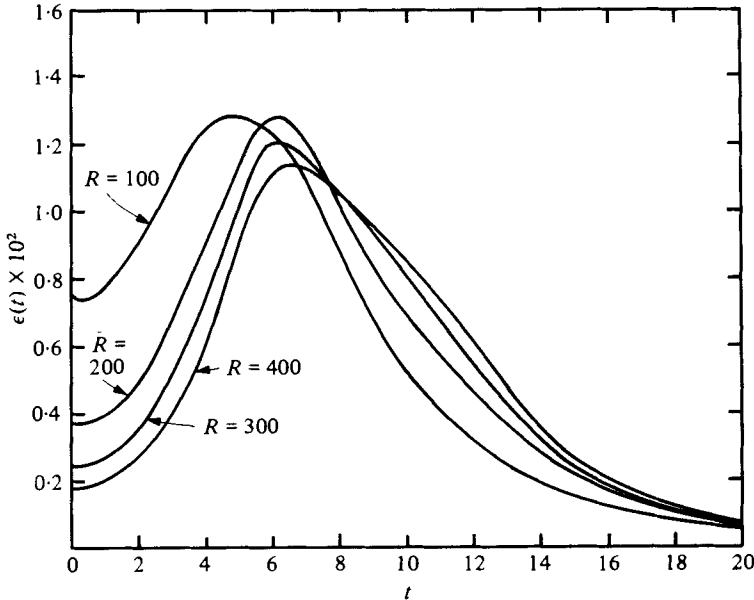


FIGURE 3. A plot of the energy dissipation rate $\epsilon(t)$ for the three-dimensional non-magnetic Taylor-Green vortex with Reynolds numbers $R = 100, 200, 300$ and 400 . The initial flow field is $\mathbf{v} = (\cos x \sin y \cos z, -\sin x \cos y \cos z, 0)$ and the Reynolds number $R = 1/\nu$.

energy dissipation is asymptotically independent of the Reynolds number as the Reynolds number approaches infinity.

The results plotted in figures 1–3 suggest that two-dimensional MHD flow does not have as strong a tendency to develop singularities as three-dimensional hydrodynamic flow. The results plotted in figures 1 and 2 do not support Pouquet’s hypothesis that $\epsilon(t)$ has a finite non-zero limit as $\nu = \mu \rightarrow 0$.

While it does not seem that $\epsilon(t)$ has a finite non-zero limit as $\nu = \mu \rightarrow 0$, the fact that $\epsilon(t)/\epsilon(0)$ achieves values much greater than 1 as $\nu = \mu \rightarrow 0$ (see figures 1 and 2) shows that vorticity is produced in two-dimensional MHD turbulence (see figure 4). When $\nu = \mu = 0.04$, the maximum enhancement of the kinetic enstrophy

$$\Sigma k^2 E^v(k, t) / \Sigma k^2 E^v(k, 0)$$

is about 2; when $\nu = \mu = 0.02$, the maximum is about $3\frac{1}{2}$; when $\nu = \mu = 0.005$, the maximum is about 10. When $\nu = \mu \lesssim 0.02$, the kinetic enstrophy reaches its maximum for $t \sim 1.5$ roughly independent of the value of $\nu = \mu$. In two-dimensional hydrodynamic unforced flow $\epsilon(t) \leq \epsilon(0)$, but the magnetic field removes this constraint. Furthermore, as $\nu = \mu \rightarrow 0$ the value of $\max \epsilon(t)/\epsilon(0)$ increases, showing that ever smaller scales of motion are produced as the Reynolds number increases.

The results that $\epsilon(t)/\epsilon(0)$ achieves values much larger than 1 and that the location of the peak of $\epsilon(t)$ is insensitive to $\nu = \mu$ suggest that a flow singularity with infinite vorticity may occur in a finite time when $\nu = \mu = 0$, as conjectured by Pouquet.

The conclusions stated above do not appear to be sensitive to the magnetic Prandtl number. In figure 4, we plot the evolution of the kinetic and magnetic enstrophies $\Sigma k^2 E^v(k)$ and $\Sigma k^2 E^m(k)$, respectively, with the initial condition (7) for several values of

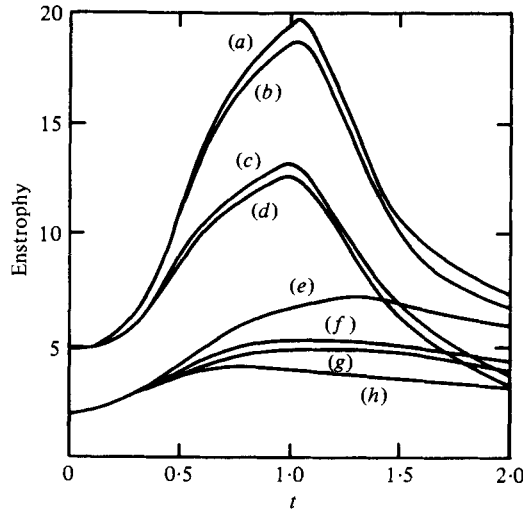


FIGURE 4. A plot of the kinetic and magnetic enstrophies $\Sigma k^2 E^v(k, t)$ and $\Sigma k^2 E^m(k, t)$, respectively, for the two-dimensional MHD flow with initial condition (7). (a) Magnetic and (e) kinetic enstrophy with $\nu = \mu = 0.02$. (b) Magnetic and (g) kinetic enstrophy with $\nu = 0.04$, $\mu = 0.02$. (c) Magnetic and (f) kinetic enstrophy with $\nu = 0.02$, $\mu = 0.04$. (d) Magnetic and (h) kinetic enstrophy with $\nu = 0.04$, $\mu = 0.04$.

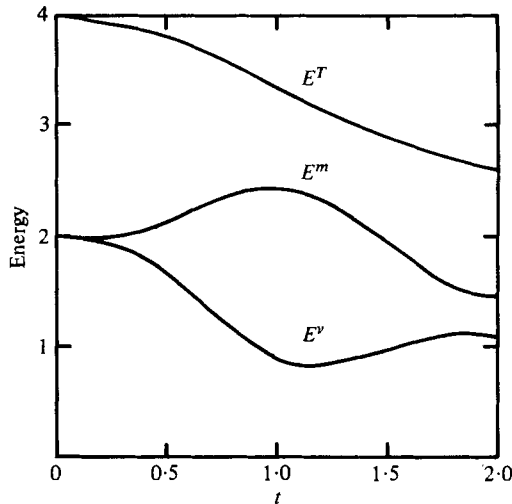


FIGURE 5. A plot of the kinetic, magnetic and total energies E^v , E^m and E^T , respectively, as functions of t for the two-dimensional MHD flow with initial condition (7) and $\nu = \mu = 0.02$.

ν and μ . Evidently production of magnetic enstrophy in this flow is governed strongly by the value of the magnetic diffusivity μ but only weakly by the viscosity ν .

In figure 5, we plot the kinetic, magnetic and total energies *vs.* t for $\nu = \mu = 0.02$. There is significant energy transfer between the kinetic and magnetic components. In the inviscid limit, this transfer must conserve both total energy and mean-square vector potential. Since $E^m = \Sigma k^2 |A(k)|^2$, transfer of magnetic vector potential out of its initial excitation band must enhance magnetic energy at the expense of kinetic energy, at least until dissipation becomes significant.

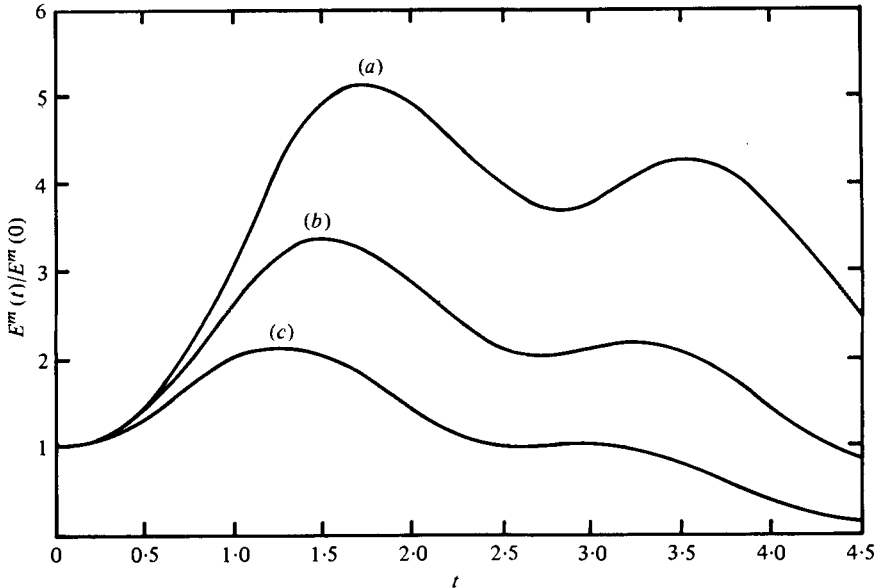


FIGURE 6. A plot of the evolution of magnetic energy $E^m(t)/E^m(0)$ in a two-dimensional MHD flow with a seed magnetic field. The initial flow is given by (7) modified by scaling the magnetic vector potential A such that $E^m(0)/E^v(0) = 10^{-4}$. (a) $\nu = \mu = 0.01$, (b) $\nu = \mu = 0.02$, (c) $\nu = \mu = 0.04$.

In figure 6, we examine the growth of a seed magnetic field. The initial flow is proportional to (7) with the amplitude of A decreased such that the initial value of E^m/E^v is 10^{-4} . As $\nu = \mu$ decreases, the maximum amplitude of E^m increases in a manner that is not inconsistent with growth to a finite level in the high Reynolds number limit.

In figures 7 and 8 we plot contours of the current j and vorticity ζ at $t = 1$ for the run with initial condition (7) and $\nu = \mu = 0.005$. In figures 9–11 we plot the streamlines of the velocity field, the contours of the magnitude $|\mathbf{h}|$ of the magnetic field and the magnetic lines of force, respectively, for the same run at $t = 1$.

The effects of the magnetic field are best exhibited by comparison of the vorticity contours plotted in figure 8 with similar vorticity contours obtained by integration of a two-dimensional non-magnetic flow. If the non-magnetic flow has the initial velocity field (7) with $\mathbf{A} = 0$, then the solution of (1)–(3) is simply

$$\mathbf{v} = (-\sin y e^{-2\nu t}, \sin x e^{-2\nu t}),$$

so the flow just decays with no nonlinear effects. On the other hand, if we choose the initial non-magnetic velocity field to be

$$\mathbf{v} = (-\sin y, \sin 2x) \quad (9)$$

then nonlinear effects are possible. In figure 12 we plot contours of vorticity ζ at $t = 1$ for the two-dimensional non-magnetic flow with $\nu = 0.005$ and initial condition (9). It is apparent that the vorticity of the MHD flow plotted in figure 8 is significantly more intermittent than that of the non-magnetic flow plotted in figure 12. This intermittency of the MHD flow is especially apparent in the contour plot of the current j (see figure 7), in which the distinctive S-shaped local structure appears in the centre of the plot.

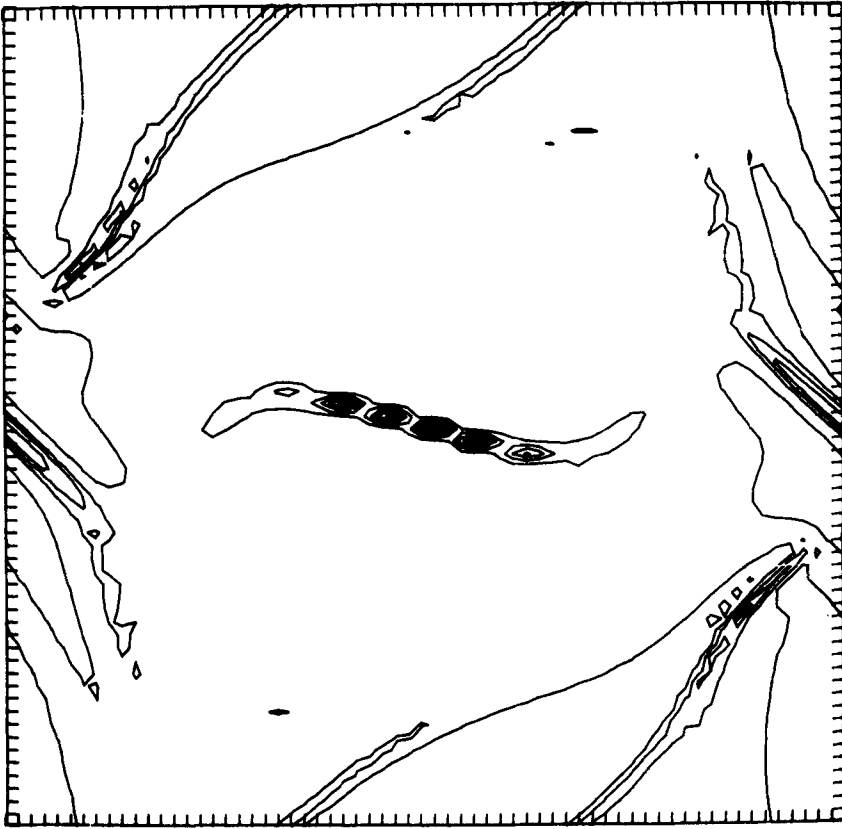


FIGURE 7. Contour plot of current $j(x, y)$ at $t = 1$ for the two-dimensional MHD flow with initial condition (7) and $\nu = \mu = 0.005$.

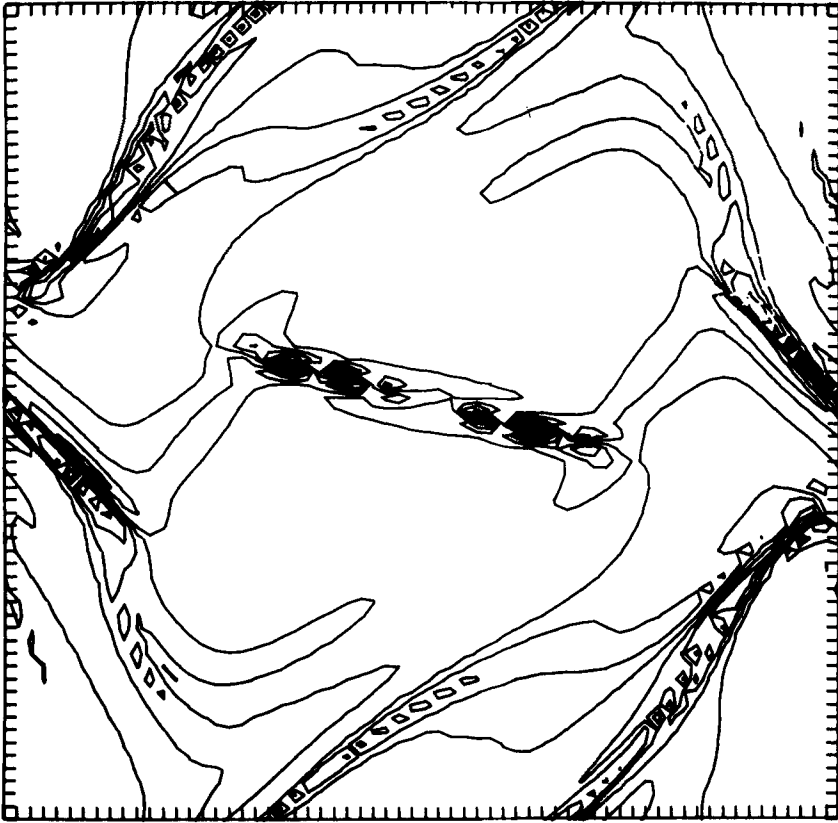


FIGURE 8. Contour plot of vorticity $\zeta(x, y)$ at $t = 1$ for the two-dimensional MHD flow with initial condition (7) and $\nu = \mu = 0.005$.

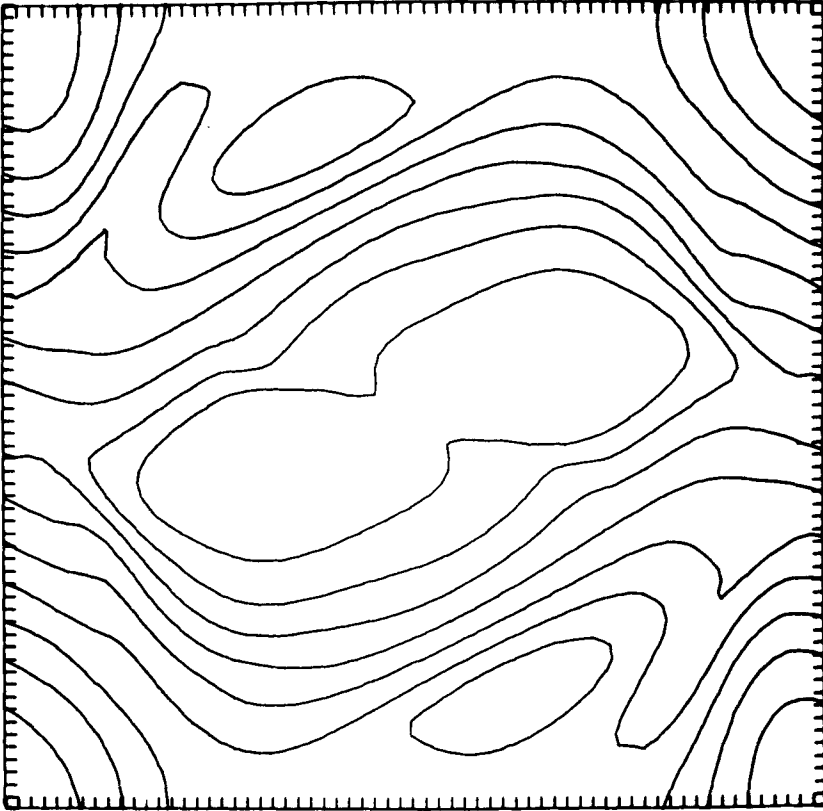


FIGURE 9. Streamlines of the velocity field at $t = 1$ for the two-dimensional MHD flow with initial condition (7) and $\nu = \mu = 0.005$.

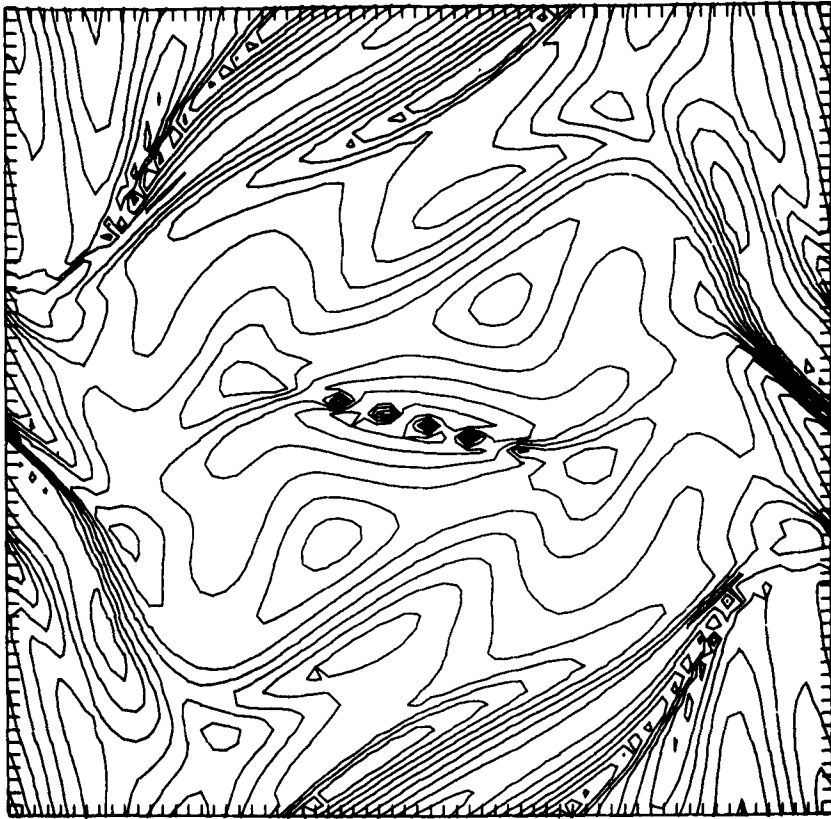


FIGURE 10. Contours of magnetic field intensity $|\mathbf{h}(x, y)|$ at $t = 1$ for the two-dimensional MHD flow with initial condition (7) and $\nu = \mu = 0.005$.

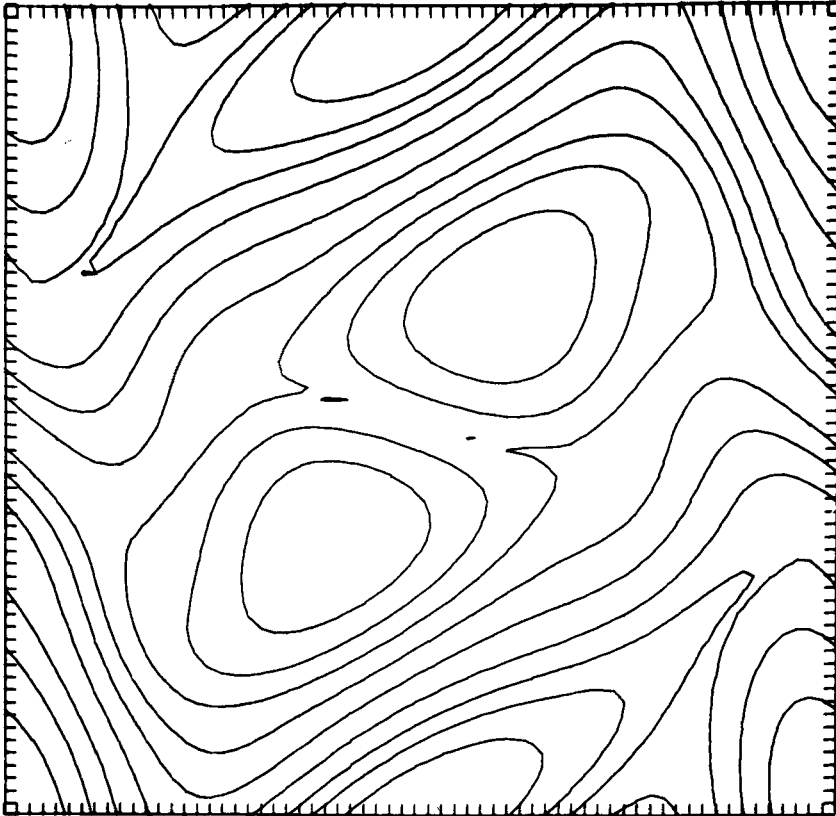


FIGURE 11. Magnetic lines of force [contours of $A(x, y)$] at $t = 1$ for the two-dimensional MHD flow with initial condition (7) and $\nu = \mu = 0.005$.

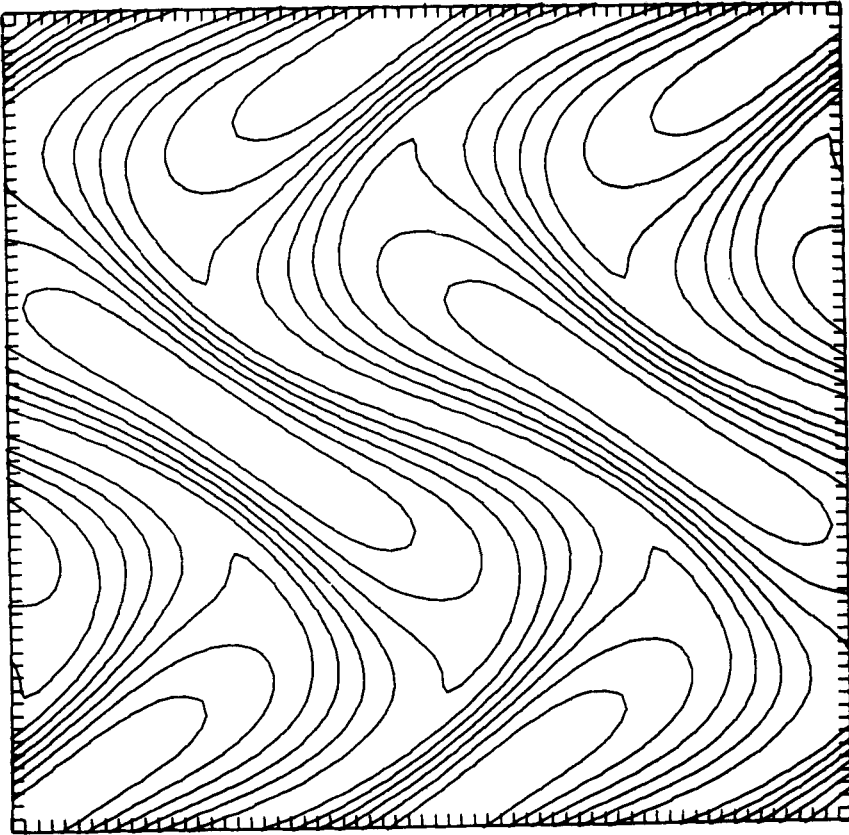


FIGURE 12. Contour plot of vorticity $\zeta(x, y)$ at $t = 1$ for the two-dimensional non-magnetic flow with initial condition (9) and $\nu = 0.005$.

4. Discussion

While all unforced solutions of (1)–(3) with $\nu, \mu > 0$ must eventually decay to zero because

$$\frac{d}{dt} \int A^2 d\mathbf{x} < 0, \quad \frac{dE}{dt} < 0$$

unless $\zeta = h = 0$, the intermediate flow states before decay can be quite complicated. Two-dimensional non-magnetic turbulence is effectively constrained by the absence of vortex stretching so no appreciable energy dissipation can occur. From the mathematical point of view, the bounds on vorticity in two-dimensional non-magnetic flow maintain the regularity of the flow for all time. On the other hand, a magnetic field can circumvent the vorticity constraint so vorticity can be produced. While two-dimensional MHD flows decay more rapidly than their non-magnetic counterparts when $\nu, \mu > 0$, they also exhibit enhanced intermittent flow structures. As $\nu = \mu \rightarrow 0$, our numerical results suggest that flow structures of arbitrarily small size are produced in a finite time, suggesting that the inviscid equations produce singularities in a finite time. This inference should be further tested by more comparisons with high resolution numerical solutions of (1)–(3).

A simple physical explanation for the production of small-scale motions by MHD flows is in order. When $\nu = \mu$ is small, an initial weak magnetic field is stretched and convected by the velocity field and thus wrapped into tight ‘ropes’ that follow closely the large-scale fluid flow. When neighbouring lines of force are thus stretched into close proximity to each other, magnetic diffusion can break the lines of force and locally reconnect them. When the lines of force snap, their tension force reacts back on the flow field to produce small eddies on top of the larger convecting ones, giving an enhanced cascade process. This argument does not give convincing proof that a singularity forms in a finite time for the inviscid MHD system because it relies on diffusion to produce small-scale motions. Evidently the dynamical process is somewhat more complicated with the mechanism just discussed responsible for only part of the observed effects.

The same kind of mechanism seems to give an enhanced cascade process, and with it enhanced small-scale structure and flow singularities, whenever the quadratic constant of motion $\int \zeta^2 d\mathbf{x}$ of inviscid two-dimensional hydrodynamic flow is destroyed by non-dissipative forces. For example, stable stratification in a Boussinesq fluid voids the vorticity constraint, so that, if the initial turbulent motion is strong enough, an enhanced cascade can take place (as will be discussed thoroughly in a later paper). Dynamical forces like those provided by magnetic fields and stable stratification have stabilizing effects on small amplitude motions but may have destabilizing effects that enhance the production of small-scale motions when applied to initially large amplitude turbulent flows.

The authors would like to thank Dr U. Frisch, Dr W. V. R. Malkus and Dr A. Pouquet for helpful discussions. This work was partially supported by the Office of Naval Research under Contract N00014-77-C-0138. The authors would also like to acknowledge use of the Computing Facility of the National Center for Atmospheric Research, Boulder, Colorado, which is supported by The National Science Foundation.

REFERENCES

- FYFE, D., JOYCE, G. & MONTGOMERY, D. 1977 *J. Plasma Phys.* **17**, 317.
- FYFE, D. & MONTGOMERY, D. 1976 *J. Plasma Phys.* **16**, 181.
- GOTTLIEB, D. & ORSZAG, S. A. 1977 *Numerical Analysis of Spectral Methods*. Philadelphia: SIAM, CBMS-NSF Monograph no. 26.
- HERRING, J. R., ORSZAG, S. A., KRAICHNAN, R. H. & FOX, D. G. 1974 *J. Fluid Mech.* **66**, 417.
- ORSZAG, S. A. 1976 Design of large hydrodynamics codes. In *Computer Science and Scientific Computing* (ed. J. Ortega), p. 191. Academic Press.
- ORSZAG, S. A. 1977 Lectures on the statistical theory of turbulence. In *Fluid Dynamics* (ed. R. Balian & J. L. Peube), p. 235. Gordon & Breach.
- POUQUET, A. 1978 *J. Fluid Mech.* **88**, 1.
- TANG, C. M. 1977 Sc.D. thesis, Department of Electrical Engineering, M.I.T., Cambridge.
- WEISS, N. O. 1966 *Proc. Roy. Soc. A* **293**, 310.
- WOLIBNER, W. 1933 *Math. Z.* **37**, 668.